

Lens Stochastic Diffraction: A Signature of Compact Structures in Gravitational-Wave Data

Miguel Zumalacárregui^{1, *}

¹*Max Planck Institute for Gravitational Physics (Albert Einstein Institute)
Am Mühlenberg 1, D-14476 Potsdam-Golm, Germany*

(Dated: April 29, 2024)

Every signal propagating through the universe is diffracted by the gravitational fields of intervening objects, aka gravitational lenses. Diffraction is most efficient when caused by compact lenses, which invariably produce additional images of a source. The signals associated with additional images are generically faint, but their collective effect may be detectable with coherent sources, such as gravitational waves (GWs), where both amplitude and phase are measured. Here, I describe *lens stochastic diffraction* (LSD): Poisson-distributed fluctuations after GW events caused by compact lenses. The amplitude and temporal distribution of these signals encode crucial information about the mass and abundance of compact lenses. Through the collective stochastic signal, LSD offers an order-of-magnitude improvement over single lens analysis for objects with mass $\gtrsim 10^3 M_\odot$. This gain can improve limits on compact dark-matter halos and allows next-generation instruments to detect supermassive black holes, given the abundance inferred from quasar luminosity studies.

I. INTRODUCTION

Gravitational lensing, the deflection of propagating signals by intervening gravitational fields, is a sensitive probe of matter distribution. It illuminates the Universe's darkest objects: black holes [1–4] and dark matter halos [5–10]. Most lensing applications to date rely on electromagnetic sources. However, the emergence of gravitational wave (GW) astronomy [11–16] provides new opportunities for gravitational lensing, which motivate detection strategies [17–22]. Given the steady improve in sensitivity, multiply imaged GW sources are bound to become a reality in the near future [23–27]. The detection of lensed GWs will provide new applications in cosmology, astrophysics and fundamental physics [28–32], including the detection and characterization of dark-matter structures [33–47].

GW lensing is highly complementary to lensed electromagnetic radiation [48–50]. As GW detectors are sensitive to field amplitude and phase (rather than energy flux), the signal strength decreases with distance (rather than distance squared), facilitating the detection of remote sources. In lensing, this scaling makes GWs more robust to demagnification, allowing the observation of faint images, including strongly deflected trajectories for sources near a massive black hole [51–53], central images of strongly lensed systems [35, 54], and systems with large lens-source angular separation [28, 47, 55–58]. The prospects of observing faint images increases significantly because the number of lenses scales with the square of source-lens separation.

In addition to loud transient signals, detectors are also sensitive to GW backgrounds, a stochastic superposition of many faint signals. An astrophysical background from unresolved mergers is expected [59], and cosmological

backgrounds could be produced by early-universe phenomena [60]. Although signals are too weak to be resolved, their existence can be inferred as an excess over instrumental noise, or by cross-correlating the output of multiple detectors [61–63].

Here, I present *lens stochastic diffraction* (LSD), a novel signature of compact structures consisting of faint counterparts present after loud GW events. These secondary signals, caused by compact lenses, follow a stochastic distribution, resembling that of GW backgrounds. I will introduce the LSD signal caused by an ensemble of point lenses, derive its time distribution and signal-to-noise ratio, and show its potential to detect compact objects, before discussing open issues and prospects.

II. LENS STOCHASTIC DIFFRACTION

A point-like gravitational lens forms at least one additional image of any source. The ratio of the lensed/unlensed flux is given by the magnification, which for an isolated point lens reads

$$\mu_I = \frac{\Delta_I^4}{\Delta_I^4 - 1} = \frac{1}{2} \pm \frac{y_l^2 + 2}{2y_l \sqrt{y_l^2 + 4}}. \quad (1)$$

Here $I = (+, -)$ labels the main/additional image and the sign corresponds to the parity. $\Delta_I = |\vec{x}_I - \vec{y}_l|$ is the image-lens angular separation: coordinates are centered around the undeflected source and $\vec{x}_I \equiv \vec{\theta}_I/\theta_E$, $\vec{y}_l \equiv \vec{\theta}_l/\theta_E$ are the image and lens position in units of the Einstein angle, $\theta_E = \sqrt{\frac{4GM_{LS}}{D_L D_S}}$. The angular diameter distances D_L , D_S , D_{LS} (for observer-lens observer-source and lens-source, respectively) are given by flat- Λ CDM cosmology [64].

The existence of a faint image near the lens is associated with a strongly deflected trajectory. At large angu-

* miguel.zumalacarregui@aei.mpg.de

lar separations, $y_l \gg 1$, the secondary image flux scales as $|\mu_-| \approx y_l^{-4}$. In typical electromagnetic sources, strong demagnification prevents the observation of additional images in generic source-lens configurations. Instead, the signal amplitude of GWs is modulated by $\sqrt{|\mu_-|} \approx y_l^{-2}$, making faint images more easily observable.

Increasing the offset y_l decreases the amplitude of individual images but increases their number: N point lenses produce at least $N + 1$ images and as many as $(N + 1)^2$ [65].¹ The enclosed average number of lenses

$$N_c(< y_l) = \kappa_c y_l^2, \quad (2)$$

depends on the line of sight via the convergence $\kappa_c = 4\pi G \Sigma_c \frac{D_{LS} D_L}{D_S}$, where Σ_c the projected surface density of compact objects. The lens number K follows a Poisson distribution $\mathcal{P}(K|N_c)$, with κ_c set by the line of sight to the source. The average convergence is [67]

$$\bar{\kappa}_c(z_S) = \frac{3}{2} f_c \Omega_{\text{DM}} H_0^2 \int_0^{z_S} dz' \frac{(1+z')^2 D_L D_{LS}}{H(z') D_S}, \quad (3)$$

where H_0 is the Hubble constant and f_c is the fraction of compact objects, relative to the dark-matter abundance Ω_{DM} and the comoving density of compact objects is assumed constant. For point lenses $\bar{\kappa}_c$ is independent of the lens' mass.

Scaling with y_l suggests that secondary images will rarely be identified individually but can be detected collectively. Fig. 1 shows the distributions of images in the sky and their amplitude and delay, for two realizations with low and high κ_c . The results are obtained from numerical solutions and assuming isolated lenses, Eq. (1). For $\kappa_c \ll 1$ at most one lens is closely aligned with the source. Then Eq. (1) describes the two brightest images, plus other secondary images with $y_k \gg 1$. The higher κ_c increases both individual magnifications and the chance of forming additional images [68–70]. Therefore, the isolated lens approximation is accurate for $\kappa_c \ll 1$ and conservative otherwise (see Fig. 3 below). Hereafter I assume that lenses can be treated as isolated.

The time distribution of secondary images encodes information about the lens mass distribution. Each secondary image arrives with a characteristic delay, which depends on the lens mass, redshift and offset as

$$t_l \approx 2GM_l(1+z_l)y_l^2 \equiv \tilde{t}_l \frac{y_l^2}{2} \quad (y_l \gg 1), \quad (4)$$

where the second equality defines a dimensionless delay. To remain in the geometric optics description, we will require that the time delays between different images satisfy $2\pi(t_i - t_j)f \gg 1$, where f is the GW frequency [50].

¹ Even more images form when lenses are distributed at different distances, because of consecutive deflections. I will neglect those and assume that all lenses can be projected onto a common lens plane by rescaling the Einstein radii [66].

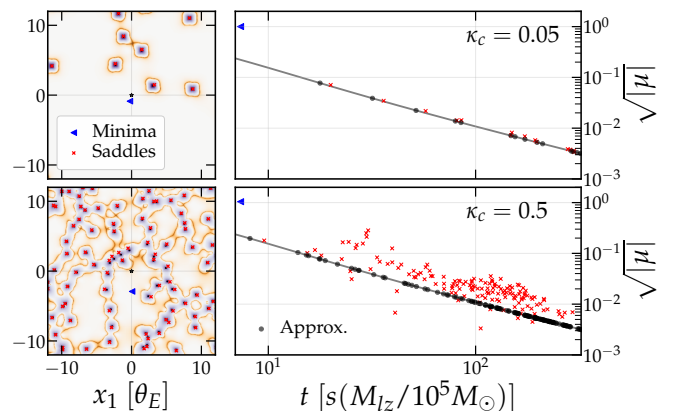


FIG. 1. Distribution of images for low (top) and high (bottom) projected lens density. **Left:** lens (dots) and images (triangles, crosses), color shows high/low magnification (orange-purple). **Right:** amplitude and arrival time of the secondary images (crosses) and the isolated-lens approximation (dots). The primary image (triangle) is shifted from $t = 0$.

A GW signal lensed by a collection of point-particles in the geometric optics regime is described by

$$h_L(t) = \sqrt{\mu_+} h_0(t) + \sum_I \sqrt{|\mu_I|} h_0^\dagger(t - t_I), \quad (5)$$

Here $\mu_+ > 1$ is the primary image magnification, not directly observable, and $h_0(t) = \sum_{p=+, \times} F_p(t) h_{0,p}(t)$ includes the detector antenna pattern. The index I labels the additional images and h_0^\dagger is the Hilbert-transform of the unlensed signal, accounting for the phase difference in negative parity images [71, 72].² Under the sparsity assumption there is one image per lens $I \rightarrow l$ and $\mu_I \approx \mu_-(y_k)$ is well approximated by Eq. (1)

The *lens stochastic diffraction* (LSD) signal is defined by the sum of additional images in Eq. (5). Although stochastic, it differs from GW backgrounds:

1. LSD is neither stationary nor Gaussian: its correlation with the primary GW signals is determined by the lens mass distribution (Eq. 4).
2. Although most GW backgrounds are isotropic, the LSD is received from the same sky localization as the main signal.
3. The waveform of individual LSD contributions is known from the resolved signal h_0 (Eq. 5), up to parameter-estimation uncertainties.

LSD also differs from the contribution on the astrophysical stochastic background from magnified high redshift sources [73–75].

² Positive parity images can be included in Eq. (5) by adding $\sum_M \sqrt{\mu_M} h_0(t - t_M) - \sum_N \sqrt{\mu_N} h_0(t - t_N)$, where M, N index secondary minima and maxima of the time delay, respectively.

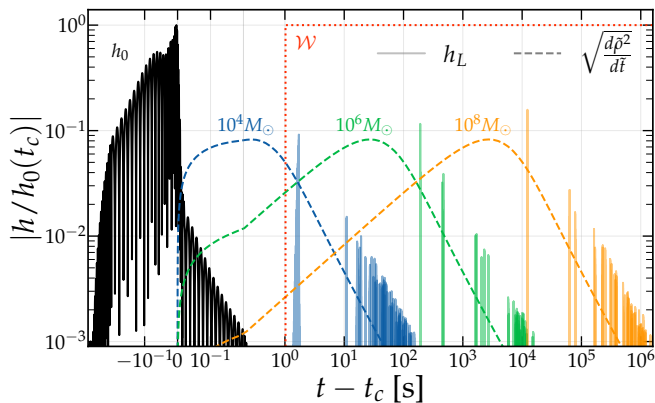


FIG. 2. Lens stochastic diffraction. Solid lines show the strain corresponding to the main image (black) and 3 different LSD realizations for different lens masses, assuming $\bar{\kappa}_c = 0.05$. Dashed lines show the average LSD amplitude, dotted line shows the window used to define the LSD signal.

Examples of LSD realizations following an $30 + 30M_\odot$ equal-mass, non-spinning merger are shown in Fig. 2 for different lens masses. The projected density $\bar{\kappa}_c = 0.05$ corresponds to a source at $z_s = 1$ with $f_c = 1$.

III. TEMPORAL DISTRIBUTION AND SIGNAL-TO-NOISE RATIO

Let us now investigate the temporal distribution and signal-to-noise ratio (SNR) of LSD. To separate LSD in Eq. (5), I will introduce a window function $\mathcal{W}(t)$ that is one for $t - t_c > T_{\min} = 1$ s after coalescence and zero elsewhere (Fig. 2). The LSD signal is $\Delta h(t) \equiv \mathcal{W}(t)h_L(t)$.

The SNR of the LSD after a GW event is then $\rho_{\text{LSD}}^2 = (\Delta h | \Delta h)$, where $(h_1 | h_2)$ is the noise-weighted inner product [76]. The LSD-SNR is

$$\frac{\rho_{\text{LSD}}^2}{\rho_0^2} = \sum_I |\mu_I| + \sum_{I \neq J} \sqrt{|\mu_I \mu_J|} M(t_I - t_J), \quad (6)$$

where $\rho_0^2 \equiv (h_0^\dagger | h_0^\dagger) = (h_0 | h_0)$ is the SNR of the unlensed event and $M(\Delta t) = \rho_0^{-2} (h_0(t) | h_0(t - \Delta t))$ is the match between different images. The first sum in Eq. (6) represents the contribution of each image after T_{\min} . The double sum accounts for interference between separate images and has zero average, since t_I 's are not correlated. Eq. (6) assumes a constant antenna pattern, a good approximation for $t_I \ll 1$ d, or $M_L \lesssim 10^7$.³

Let us now study the average LSD-SNR relative to the unlensed event, $\tilde{\rho}_{\text{LSD}}^2 \equiv \langle \rho_{\text{LSD}}^2 \rangle / \rho_0^2$. The sum over images is replaced by integrals weighted by the lens number

³ For large t_I, M_L the average LSD-SNR will be slightly lower due to selection bias, as a detection threshold favors events with $F_p(t_c) > \langle F_p \rangle$.

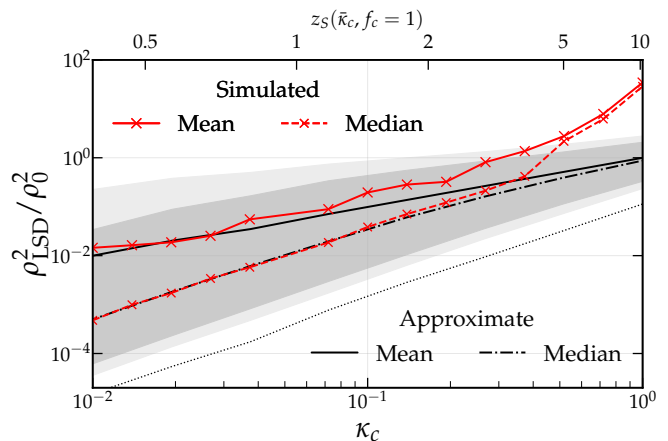


FIG. 3. LSD-SNR distribution as a function of convergence. The mean and median of simulations (red) is larger than the isolated lens approximation (black) for $\kappa_c \gtrsim 0.1$. The 90%, 98% c.i. and minimum values of the approximate distribution are also shown (resp. gray bands and dotted line). The top scale shows the redshift at which $\bar{\kappa}_c = \kappa_c$ for $f_c = 1$, Eq. (3).

density $\sum_I \rightarrow \int dt \frac{dN_c}{dt} \mathcal{W}(t)$. Assuming isolated lenses, the average relative differential LSD-SNR is

$$\frac{d\tilde{\rho}_{\text{LSD}}^2}{dt dM} = \mathcal{W}(t) \frac{df_c}{dM} \int_0^{z_s} dz' dy^2 \frac{d\bar{\kappa}_c}{dz'} | \mu_- | (y) \delta(t - t(y)), \quad (7)$$

Here $\frac{d\bar{\kappa}_c}{dz'}$ is the derivative of Eq. (3), $\frac{df_c}{dM}$ is the lens mass function and the average lens density has been used (Eq. 2). The magnification and time delay are evaluated as for an isolated lens, cf. Eqs. (1,4).

The total LSD-SNR is the integral of Eq. (7) over time and lens mass. If $\mathcal{W}(t) \rightarrow 1$ it simplifies to

$$\tilde{\rho}_{\text{LSD}}^2 = 2\bar{\kappa}_c \int dy y | \mu_- | (y) \approx \bar{\kappa}_c. \quad (8)$$

Note that including $\mathcal{W}(t)$ will add a dependence on both the lens' mass and the source redshift, which is important for $M \lesssim 10^4 M_\odot$ (cf. Fig. 2). Similarly, an upper limit on the time delays considered needs to be included, which will affect the sensitivity to high mass objects.

The distribution of the LSD-SNR depends strongly on κ_c , whose summary statistics are shown in Fig. 3. For the isolated lens approximation, the mean of random realizations agrees with Eq. (8). At low κ_c , the distribution is skewed, as the median $\propto \kappa_c^2 \ll \tilde{\rho}^2$ deviates from the mean due to rare events with high $\tilde{\rho}_{\text{LSD}}$ ($y_i \ll 1$). The LSD-SNR distribution was obtained numerically, using Eq. (6) (only first sum) for 100–1000 random realizations at each value of κ_c . The simulated LSD-SNR becomes larger than the approximate value of $\kappa_c \gtrsim 0.1$ due to the formation of additional images and collective lensing effects, confirming that the isolated lens approximation is conservative.

IV. OBSERVATIONAL PROSPECTS

Let us now estimate the sensitivity of ground detectors to LSD given the abundance of compact objects, f_c . The rate calculation follows Refs. [77, 78]. I consider the LIGO-Virgo-KAGRA (LVK) detector network at O5 sensitivity, the Einstein Telescope (ET) [79] and a single Cosmic Explorer (CE) interferometer [80]. I will consider only non-spinning and quasicircular black hole mergers.

The detection rate and the average LSD-SNR for source catalogue are given by

$$\dot{N} = \mathcal{R}_0 \int d\vec{\theta} \frac{dP}{d\vec{\theta}} \int dz \frac{dV}{dz} P_{\text{det}} f_{\text{SFR}}, \quad (9)$$

$$\bar{\rho}_{\text{LSD}}^2 = \mathcal{R}_0 \int d\vec{\theta} \frac{dP}{d\vec{\theta}} \int dz \bar{\kappa}_c \frac{dV}{dz} \bar{w}^2 \rho_{\text{opt}}^2 P_{\text{det}} f_{\text{SFR}}. \quad (10)$$

Here $\vec{\theta} = m_1, m_2$ are the binary intrinsic parameters and $\frac{dP}{d\vec{\theta}}$ is the population model given by the ‘‘power law + peak’’ model (fiducial parameters in Ref. [81]). The volume element, $\frac{dV}{dz}$ is that of flat Λ CDM [64] and the source distribution, $f_{\text{SFR}}(z)$, follows the star formation rate [82], with a normalization $\mathcal{R}_0 = 30 \text{Gpc}^{-3} \text{yr}^{-1}$ [83]. $P_{\text{det}}(w)$ is the fraction of detected sources, which depends on the ratio of the detection threshold to the optimal SNR $w(z) = \rho_{\text{th}}/\rho_{\text{opt}}(z, \vec{\theta})$, with $\rho_{\text{th}} = 8$. P_{det} and ρ_{opt} are obtained using `gwfast` [84, 85]. The LSD-SNR depends on the second moment $\bar{w}^2 = \int dw w^2 P_{\text{det}}(w)$ and $\bar{\kappa}_c(z) \propto f_c$.

The mass of the lens affects the total LSD-SNR by changing the arrival time of secondary signals (Eq. 4) relative to T_{min} in the window function. Eq. (10) is valid for $4GM_l(1+z_l) \gg T_{\text{min}}$: The effect of M_l is estimated by multiplying $\bar{\rho}_{\text{LSD}}^2$ by $\frac{1}{\bar{\rho}^2} \int_{T_{\text{min}}}^{\infty} \frac{d\bar{\rho}^2}{dt} dt$ (Eq. 7), assuming $z_S = 1$ (below the typical source redshift for future detectors). Note that LSD includes lensed events where secondary signals are individually detected, $\rho_0 \sqrt{|\mu_-|} > \rho_{\text{th}}$.

Detection of the LSD or its absence provides competitive limits on the abundance of compact objects with $M \gtrsim 10^3 M_\odot$. Fig. 4 shows current lensing constraints from quasars [86], stars [87–89], type Ia supernovae [90] and GWs from LVK O3a [38], as well as expected limits from fast radio bursts (FRBs) [91], GWs under single-lens analysis [39, 40] and with LSD (90% c.l. and 1 year of observation). The lensing limits for $M \gtrsim 300 M_\odot$ will be dominated by lensed GWs in the near future. Single-lens analyzes are more constraining for objects with $M \sim (8\pi Gf)^{-1}$. The improvement is due to wave-optics lensing effects, which are excluded from the LSD by signal windowing. Instead, for $M \gg (8\pi Gf)^{-1}$, LSD incorporates information from low-amplitude images, representing an order-of-magnitude gain in sensitivity.

LSD constraints are complementary to other probes of compact objects and dark matter. For comparison, Fig. 4 shows two model-dependent limits for primordial black holes: current cosmic microwave background (CMB) accretion limits [92] and forecasted limits from merger rate

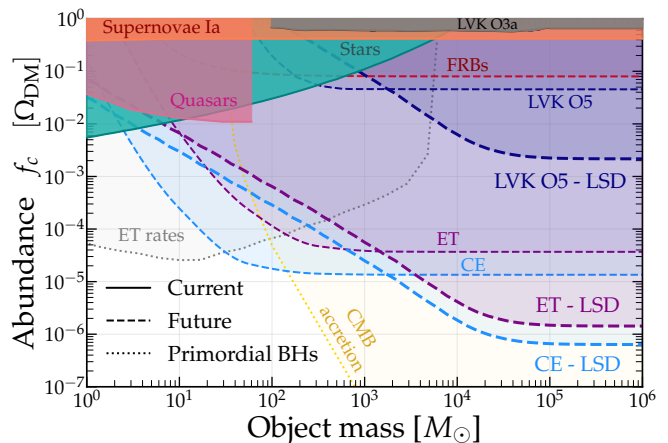


FIG. 4. Potential of the LSD to constrain the abundance of compact objects (thick dashed) for LVK-O5 (blue), ET (purple) and CE (light blue). For high masses, the LSD leads to a factor $\sim 10^2 - 10^5$ improvement over existing lensing limits (solid). The gain is also substantial relative to the standard GW lensing analysis by the same network (thin dashed). Model-dependent results for primordial black holes (dotted) are shown for comparison, see text.

by ET [93]. Although stringent, these limits require dark matter to be very compact and be present before recombination. In contrast, LSD probes extended structures, such as compact dark-matter halos and black holes of astrophysical origin. Then, the finite size prevents the formation of additional images for offsets $y \gtrsim \Delta x^{-1}$, where $\Delta x = \frac{R_L}{D_L \theta_E}$ is the object’s size over its Einstein radius. This allows objects with $R_L \lesssim 1 \text{pc} (M_L/10^4 M_\odot)^{1/2}$ to be probed by LSD, $\sim 10^3$ times larger than the CMB [94]. The effect of lens size can be determined accurately by changing $\mu(y)$ in Eq. (7).⁴

Two potential targets of LSD are supermassive black holes (SMBHs) and compact dark-matter halos. Both ET and CE have the potential to probe SMBHs via LSD, with $\Omega_{\text{SMBHs}}/\Omega_{\text{DM}} \sim 1.5 \cdot 10^{-5}$ estimated from the quasar luminosity function [95, 96]. Other systems, such as lensed gamma-ray bursts, suggest the existence of compact lenses whose mass and abundance could be further probed by LSD [97–99]. Beyond detection, the temporal distribution of the LSD (Eq. 7) can be used to constrain the mass function of compact structures.

⁴ A cutoff for secondary images in y_l causes a drop in the LSD after a characteristic delay (Eq. 4), whose observation can constrain the lens properties. Non-singular lenses also form central images [35], whose short time delay may introduce wave-optics distortions. The analysis here can be extended by replacing h_0^\dagger with the distorted waveform from the extended lens.

V. DISCUSSION

Lens stochastic diffraction (LSD) is a new signature of compact lenses in GW data, sensitive to objects with $M \gg (Gf)^{-1}$. After a GW event, it manifests itself as multiple secondary signals, each a phase-shifted faint copy of the main event (Figs. 1,2). The delays follow a Poisson distribution, depending on the object's mass and abundance. Secondary signals can only be individually identified if a lens is closely aligned with the source. However, considering these signals collectively enables LSD to effectively probe compact objects.

LSD can detect compact lenses more efficiently than single lens analysis of GWs and electromagnetic transients for $M_L \gtrsim 10^2 - 10^3 M_\odot$ (Fig. 4). While the CMB is a more powerful test of primordial black holes, LSD is sensitive compact dark-matter halos and objects formed after recombination. It complements existing methods [94, 100, 101] and can target specific theories, such as compact axion structures [102]. Beyond ground GW interferometers, space detectors like LISA [103, 104] can leverage the high SNR and redshift of massive black hole mergers.

Several challenges must be addressed to extract the LSD signature from real data. Uncertainties in the main signal (from parameter estimation, differences in the lens model) will degrade the SNR by the mismatch between the true and assumed waveforms. Astrophysical GW

backgrounds provide a source of confusion with LDS signals. Among the unresolved events, some will have intrinsic parameters and sky localization similar enough to the main signal to be confused with LSD (analogous to the issue of false alarm probability in strongly imaged events [26, 105]). The LSD can be distinguished by exploiting the correlation with resolved signals, which are absent in stochastic backgrounds. Further improvements are expected by incorporating techniques for stochastic backgrounds that leverage waveform information [106–109]. These methods will alleviate the impact of data glitches and contamination from GW backgrounds.

LSD has interesting connections to strong lensing and microlensing. The time distribution of secondary images (whether they appear after, around, or before the primary signal) could be used to reveal the image type [110, 111]. Most interestingly, extending the analysis to the wave-optics regime will provide insights into lighter lenses, including signatures of stars in multiply imaged GWs [112–120].

ACKNOWLEDGMENTS

I am very grateful to S. Goyal, S. Savastano and H. Villarrubia-Rojo for comments on the manuscript, to G. Brando, J. Gair, G. Tambalo and Y. Wang for discussions and Han Gil Choi also for sharing the results of Ref. [40]. This work relied on `Gwfast` [84, 85], `PBHbounds` [121], `Astropy` [122–124], `Numpy` [125] and `Scipy` [126].

-
- [1] K. C. Sahu *et al.* (OGLE, MOA, PLANET, μ FUN, MiNDSTeP Consortium, RoboNet), An Isolated Stellar-mass Black Hole Detected through Astrometric Microlensing, *Astrophys. J.* **933**, 83 (2022), arXiv:2201.13296 [astro-ph.SR].
 - [2] C. Y. Lam *et al.*, An Isolated Mass-gap Black Hole or Neutron Star Detected with Astrometric Microlensing, *Astrophys. J. Lett.* **933**, L23 (2022), arXiv:2202.01903 [astro-ph.GA].
 - [3] J. W. Nightingale *et al.*, Abell 1201: detection of an ultramassive black hole in a strong gravitational lens, *Mon. Not. Roy. Astron. Soc.* **521**, 3298 (2023), arXiv:2303.15514 [astro-ph.GA].
 - [4] L. Wyrzykowski *et al.*, Black Hole, Neutron Star and White Dwarf Candidates from Microlensing with OGLE-III, *Mon. Not. Roy. Astron. Soc.* **458**, 3012 (2016), arXiv:1509.04899 [astro-ph.SR].
 - [5] S. Vegetti *et al.*, Strong gravitational lensing as a probe of dark matter, (2023), arXiv:2306.11781 [astro-ph.CO].
 - [6] R. Massey, T. Kitching, and J. Richard, The dark matter of gravitational lensing, *Rept. Prog. Phys.* **73**, 086901 (2010), arXiv:1001.1739 [astro-ph.CO].
 - [7] D. Clowe, A. Gonzalez, and M. Markevitch, Weak lensing mass reconstruction of the interacting cluster 1E0657-558: Direct evidence for the existence of dark matter, *Astrophys. J.* **604**, 596 (2004), arXiv:astro-ph/0312273.
 - [8] S. Vegetti, D. J. Lagattuta, J. P. McKean, M. W. Auger, C. D. Fassnacht, and L. V. E. Koopmans, Gravitational detection of a low-mass dark satellite at cosmological distance, *Nature* **481**, 341 (2012), arXiv:1201.3643 [astro-ph.CO].
 - [9] Y. D. Hezaveh *et al.*, Detection of lensing substructure using ALMA observations of the dusty galaxy SDP.81, *Astrophys. J.* **823**, 37 (2016), arXiv:1601.01388 [astro-ph.CO].
 - [10] A. Diaz Rivero, F.-Y. Cyr-Racine, and C. Dvorkin, Power spectrum of dark matter substructure in strong gravitational lenses, *Phys. Rev. D* **97**, 023001 (2018), arXiv:1707.04590 [astro-ph.CO].
 - [11] B. P. Abbott *et al.* (LIGO Scientific, Virgo), Observation of Gravitational Waves from a Binary Black Hole Merger, *Phys. Rev. Lett.* **116**, 061102 (2016), arXiv:1602.03837 [gr-qc].
 - [12] B. P. Abbott *et al.* (LIGO Scientific, Virgo), GWTC-1: A Gravitational-Wave Transient Catalog of Compact Binary Mergers Observed by LIGO and Virgo during the First and Second Observing Runs, *Phys. Rev. X* **9**, 031040 (2019), arXiv:1811.12907 [astro-ph.HE].
 - [13] R. Abbott *et al.* (KAGRA, VIRGO, LIGO Scientific), GWTC-3: Compact Binary Coalescences Observed by LIGO and Virgo during the Second Part of the Third Observing Run, *Phys. Rev. X* **13**, 041039 (2023),

- arXiv:2111.03606 [gr-qc].
- [14] A. H. Nitz, S. Kumar, Y.-F. Wang, S. Kastha, S. Wu, M. Schäfer, R. Dhurkunde, and C. D. Capano, 4-OGC: Catalog of Gravitational Waves from Compact Binary Mergers, *Astrophys. J.* **946**, 59 (2023), arXiv:2112.06878 [astro-ph.HE].
 - [15] S. Olsen, T. Venumadhav, J. Mushkin, J. Roulet, B. Zackay, and M. Zaldarriaga, New binary black hole mergers in the LIGO-Virgo O3a data, *Phys. Rev. D* **106**, 043009 (2022), arXiv:2201.02252 [astro-ph.HE].
 - [16] A. K. Mehta, S. Olsen, D. Wadekar, J. Roulet, T. Venumadhav, J. Mushkin, B. Zackay, and M. Zaldarriaga, New binary black hole mergers in the LIGO-Virgo O3b data, (2023), arXiv:2311.06061 [gr-qc].
 - [17] O. A. Hannuksela, K. Haris, K. K. Y. Ng, S. Kumar, A. K. Mehta, D. Keitel, T. G. F. Li, and P. Ajith, Search for gravitational lensing signatures in LIGO-Virgo binary black hole events, *Astrophys. J. Lett.* **874**, L2 (2019), arXiv:1901.02674 [gr-qc].
 - [18] C. McIsaac, D. Keitel, T. Collett, I. Harry, S. Mozzon, O. Edy, and D. Bacon, Search for strongly lensed counterpart images of binary black hole mergers in the first two LIGO observing runs, *Phys. Rev. D* **102**, 084031 (2020), arXiv:1912.05389 [gr-qc].
 - [19] L. Dai, B. Zackay, T. Venumadhav, J. Roulet, and M. Zaldarriaga, Search for Lensed Gravitational Waves Including Morse Phase Information: An Intriguing Candidate in O2, (2020), arXiv:2007.12709 [astro-ph.HE].
 - [20] A. K. Y. Li, J. C. L. Chan, H. Fong, A. H. Y. Chong, A. J. Weinstein, and J. M. Ezquiaga, TESLA-X: An effective method to search for sub-threshold lensed gravitational waves with a targeted population model, (2023), arXiv:2311.06416 [gr-qc].
 - [21] R. Abbott *et al.* (LIGO Scientific, VIRGO, KAGRA), Search for gravitational-lensing signatures in the full third observing run of the LIGO-Virgo network, (2023), arXiv:2304.08393 [gr-qc].
 - [22] J. Janquart *et al.*, Follow-up analyses to the O3 LIGO–Virgo–KAGRA lensing searches, *Mon. Not. Roy. Astron. Soc.* **526**, 3832 (2023), arXiv:2306.03827 [gr-qc].
 - [23] L. Dai, T. Venumadhav, and K. Sigurdson, Effect of lensing magnification on the apparent distribution of black hole mergers, *Phys. Rev. D* **95**, 044011 (2017), arXiv:1605.09398 [astro-ph.CO].
 - [24] K. K. Y. Ng, K. W. K. Wong, T. Broadhurst, and T. G. F. Li, Precise LIGO Lensing Rate Predictions for Binary Black Holes, *Phys. Rev. D* **97**, 023012 (2018), arXiv:1703.06319 [astro-ph.CO].
 - [25] M. Oguri, Effect of gravitational lensing on the distribution of gravitational waves from distant binary black hole mergers, *Mon. Not. Roy. Astron. Soc.* **480**, 3842 (2018), arXiv:1807.02584 [astro-ph.CO].
 - [26] A. R. A. C. Wierda, E. Wempe, O. A. Hannuksela, L. e. V. E. Koopmans, and C. Van Den Broeck, Beyond the Detector Horizon: Forecasting Gravitational-Wave Strong Lensing, *Astrophys. J.* **921**, 154 (2021), arXiv:2106.06303 [astro-ph.HE].
 - [27] G. P. Smith, A. Robertson, G. Mahler, M. Nicholl, D. Ryczanowski, M. Bianconi, K. Sharon, R. Massey, J. Richard, and M. Jauzac, Discovering gravitationally lensed gravitational waves: predicted rates, candidate selection, and localization with the Vera Rubin Observatory, *Mon. Not. Roy. Astron. Soc.* **520**, 702 (2023), arXiv:2204.12977 [astro-ph.HE].
 - [28] R. Takahashi and T. Nakamura, Wave effects in gravitational lensing of gravitational waves from chirping binaries, *Astrophys. J.* **595**, 1039 (2003), arXiv:astro-ph/0305055.
 - [29] F. Xu, J. M. Ezquiaga, and D. E. Holz, Please Repeat: Strong Lensing of Gravitational Waves as a Probe of Compact Binary and Galaxy Populations, *Astrophys. J.* **929**, 9 (2022), arXiv:2105.14390 [astro-ph.CO].
 - [30] S. Jana, S. J. Kapadia, T. Venumadhav, and P. Ajith, Cosmography Using Strongly Lensed Gravitational Waves from Binary Black Holes, *Phys. Rev. Lett.* **130**, 261401 (2023), arXiv:2211.12212 [astro-ph.CO].
 - [31] S. Goyal, K. Haris, A. K. Mehta, and P. Ajith, Testing the nature of gravitational-wave polarizations using strongly lensed signals, *Phys. Rev. D* **103**, 024038 (2021), arXiv:2008.07060 [gr-qc].
 - [32] S. Goyal, A. Vijaykumar, J. M. Ezquiaga, and M. Zumalacáregui, Probing lens-induced gravitational-wave birefringence as a test of general relativity, *Phys. Rev. D* **108**, 024052 (2023), arXiv:2301.04826 [gr-qc].
 - [33] J. M. Diego, Constraining the abundance of primordial black holes with gravitational lensing of gravitational waves at LIGO frequencies, *Phys. Rev. D* **101**, 123512 (2020), arXiv:1911.05736 [astro-ph.CO].
 - [34] H. Gil Choi, C. Park, and S. Jung, Small-scale shear: peeling off diffuse subhalos with gravitational waves, (2021), arXiv:2103.08618 [astro-ph.CO].
 - [35] G. Tambalo, M. Zumalacáregui, L. Dai, and M. H.-Y. Cheung, Gravitational wave lensing as a probe of halo properties and dark matter, (2022), arXiv:2212.11960 [astro-ph.CO].
 - [36] J. Gais, K. K. Y. Ng, E. Seo, K. W. K. Wong, and T. G. F. Li, Inferring the Intermediate-mass Black Hole Number Density from Gravitational-wave Lensing Statistics, *Astrophys. J. Lett.* **932**, L4 (2022), arXiv:2201.01817 [gr-qc].
 - [37] P. Christian, S. Vitale, and A. Loeb, Detecting Stellar Lensing of Gravitational Waves with Ground-Based Observatories, *Phys. Rev. D* **98**, 103022 (2018), arXiv:1802.02586 [astro-ph.HE].
 - [38] S. Basak, A. Ganguly, K. Haris, S. Kapadia, A. K. Mehta, and P. Ajith, Constraints on Compact Dark Matter from Gravitational Wave Microlensing, *Astrophys. J. Lett.* **926**, L28 (2022), arXiv:2109.06456 [gr-qc].
 - [39] S. Jung and C. S. Shin, Gravitational-Wave Fringes at LIGO: Detecting Compact Dark Matter by Gravitational Lensing, *Phys. Rev. Lett.* **122**, 041103 (2019), arXiv:1712.01396 [astro-ph.CO].
 - [40] H. Gil Choi, S. Jung, P. Lu, and V. Takhistov, Co-Existence Test of Primordial Black Holes and Particle Dark Matter, (2023), arXiv:2311.17829 [astro-ph.CO].
 - [41] M. Oguri and R. Takahashi, Probing Dark Low-mass Halos and Primordial Black Holes with Frequency-dependent Gravitational Lensing Dispersions of Gravitational Waves, *Astrophys. J.* **901**, 58 (2020), arXiv:2007.01936 [astro-ph.CO].
 - [42] M. Oguri and R. Takahashi, Amplitude and phase fluctuations of gravitational waves magnified by strong gravitational lensing, *Phys. Rev. D* **106**, 043532 (2022), arXiv:2204.00814 [astro-ph.CO].
 - [43] M. Fairbairn, J. Urrutia, and V. Vaskonen, Microlensing of gravitational waves by dark matter structures, (2022), arXiv:2210.13436 [astro-ph.CO].
 - [44] J. Urrutia and V. Vaskonen, Lensing of gravitational

- waves as a probe of compact dark matter, *Mon. Not. Roy. Astron. Soc.* **509**, 1358 (2021), [arXiv:2109.03213 \[astro-ph.CO\]](#).
- [45] J. Urrutia, V. Vaskonen, and H. Veermäe, Gravitational wave microlensing by dressed primordial black holes, *Phys. Rev. D* **108**, 023507 (2023), [arXiv:2303.17601 \[astro-ph.CO\]](#).
- [46] J. Urrutia and V. Vaskonen, The dark timbre of gravitational waves, (2024), [arXiv:2402.16849 \[gr-qc\]](#).
- [47] S. Savastano, G. Tambalo, H. Villarrubia-Rojo, and M. Zumalacárregui, Weakly Lensed Gravitational Waves: Probing Cosmic Structures with Wave-Optics Features, (2023), [arXiv:2306.05282 \[gr-qc\]](#).
- [48] C. Leung, D. Jow, P. Saha, L. Dai, M. Oguri, and L. V. E. Koopmans, Wave Mechanics, Interference, and Decoherence in Strong Gravitational Lensing, (2023), [arXiv:2304.01202 \[astro-ph.HE\]](#).
- [49] C. Copi and G. D. Starkman, Gravitational Glint: Detectable Gravitational Wave Tails from Stars and Compact Objects, *Phys. Rev. Lett.* **128**, 251101 (2022), [arXiv:2201.03684 \[gr-qc\]](#).
- [50] G. Tambalo, M. Zumalacárregui, L. Dai, and M. H.-Y. Cheung, Lensing of gravitational waves: efficient wave-optics methods and validation with symmetric lenses, (2022), [arXiv:2210.05658 \[gr-qc\]](#).
- [51] B. Kocsis, High Frequency Gravitational Waves from Supermassive Black Holes: Prospects for LIGO-Virgo Detections, *Astrophys. J.* **763**, 122 (2013), [arXiv:1211.6427 \[astro-ph.HE\]](#).
- [52] L. Gondán and B. Kocsis, Astrophysical gravitational-wave echoes from galactic nuclei, *Mon. Not. Roy. Astron. Soc.* **515**, 3299 (2022), [arXiv:2110.09540 \[astro-ph.HE\]](#).
- [53] M. A. Oancea, R. Stiskalek, and M. Zumalacárregui, Probing general relativistic spin-orbit coupling with gravitational waves from hierarchical triple systems, (2023), [arXiv:2307.01903 \[gr-qc\]](#).
- [54] Y. D. Hezaveh, P. J. Marshall, and R. D. Blandford, Probing the inner kpc of massive galaxies with strong gravitational lensing, *Astrophys. J. Lett.* **799**, L22 (2015), [arXiv:1501.01757 \[astro-ph.GA\]](#).
- [55] Z. Gao, X. Chen, Y.-M. Hu, J.-D. Zhang, and S.-J. Huang, A higher probability of detecting lensed supermassive black hole binaries by LISA, *Mon. Not. Roy. Astron. Soc.* **512**, 1 (2022), [arXiv:2102.10295 \[astro-ph.CO\]](#).
- [56] M. Çalıřkan, L. Ji, R. Cotesta, E. Berti, M. Kamionkowski, and S. Marsat, Observability of lensing of gravitational waves from massive black hole binaries with LISA, (2022), [arXiv:2206.02803 \[astro-ph.CO\]](#).
- [57] S. Savastano, F. Vernizzi, and M. Zumalacárregui, Through the lens of Sgr A*: identifying strongly lensed Continuous Gravitational Waves beyond the Einstein radius, (2022), [arXiv:2212.14697 \[gr-qc\]](#).
- [58] M. Çalıřkan, N. Anil Kumar, L. Ji, J. M. Ezquiaga, R. Cotesta, E. Berti, and M. Kamionkowski, Probing wave-optics effects and dark-matter subhalos with lensing of gravitational waves from massive black holes, (2023), [arXiv:2307.06990 \[astro-ph.CO\]](#).
- [59] T. Regimbau, The Quest for the Astrophysical Gravitational-Wave Background with Terrestrial Detectors, *Symmetry* **14**, 270 (2022).
- [60] C. Caprini and D. G. Figueroa, Cosmological Back-grounds of Gravitational Waves, *Class. Quant. Grav.* **35**, 163001 (2018), [arXiv:1801.04268 \[astro-ph.CO\]](#).
- [61] N. Christensen, Stochastic Gravitational Wave Backgrounds, *Rept. Prog. Phys.* **82**, 016903 (2019), [arXiv:1811.08797 \[gr-qc\]](#).
- [62] A. I. Renzini, B. Goncharov, A. C. Jenkins, and P. M. Meyers, Stochastic Gravitational-Wave Backgrounds: Current Detection Efforts and Future Prospects, *Galaxies* **10**, 34 (2022), [arXiv:2202.00178 \[gr-qc\]](#).
- [63] N. van Remortel, K. Janssens, and K. Turbang, Stochastic gravitational wave background: Methods and implications, *Prog. Part. Nucl. Phys.* **128**, 104003 (2023), [arXiv:2210.00761 \[gr-qc\]](#).
- [64] N. Aghanim *et al.* (Planck), Planck 2018 results. VI. Cosmological parameters, *Astron. Astrophys.* **641**, A6 (2020), [Erratum: *Astron. Astrophys.* 652, C4 (2021)], [arXiv:1807.06209 \[astro-ph.CO\]](#).
- [65] H. J. Witt, Investigation of high amplification events in light curves of gravitationally lensed quasars., "Astron. Astrophys." **236**, 311 (1990).
- [66] A. Çagan Şengül, A. Tsang, A. Diaz Rivero, C. Dvorkin, H.-M. Zhu, and U. Seljak, Quantifying the line-of-sight halo contribution to the dark matter convergence power spectrum from strong gravitational lenses, *Phys. Rev. D* **102**, 063502 (2020), [arXiv:2006.07383 \[astro-ph.CO\]](#).
- [67] P. Schneider, J. Ehlers, and E. E. Falco, *Gravitational Lenses* (1992).
- [68] N. Katz, S. Balbus, and B. Paczynski, Random Scattering Approach to Gravitational Microlensing, *Astrophys. J.* **306**, 2 (1986).
- [69] T. Venumadhav, L. Dai, and J. Miralda-Escudé, Microlensing of Extremely Magnified Stars near Caustics of Galaxy Clusters, *Astrophys. J.* **850**, 49 (2017), [arXiv:1707.00003 \[astro-ph.CO\]](#).
- [70] M. Pascale and L. Dai, New Approximation of Magnification Statistics for Random Microlensing of Magnified Sources, (2021), [arXiv:2104.12009 \[astro-ph.GA\]](#).
- [71] L. Dai and T. Venumadhav, On the waveforms of gravitationally lensed gravitational waves, (2017), [arXiv:1702.04724 \[gr-qc\]](#).
- [72] J. M. Ezquiaga, D. E. Holz, W. Hu, M. Lagos, and R. M. Wald, Phase effects from strong gravitational lensing of gravitational waves, *Phys. Rev. D* **103**, 064047 (2021), [arXiv:2008.12814 \[gr-qc\]](#).
- [73] R. Busicchio, C. J. Moore, G. Pratten, P. Schmidt, M. Bianconi, and A. Vecchio, Constraining the lensing of binary black holes from their stochastic background, *Phys. Rev. Lett.* **125**, 141102 (2020), [arXiv:2006.04516 \[astro-ph.CO\]](#).
- [74] R. Busicchio, C. J. Moore, G. Pratten, P. Schmidt, and A. Vecchio, Constraining the lensing of binary neutron stars from their stochastic background, *Phys. Rev. D* **102**, 081501 (2020), [arXiv:2008.12621 \[astro-ph.HE\]](#).
- [75] S. Mukherjee, T. Broadhurst, J. M. Diego, J. Silk, and G. F. Smoot, Inferring the lensing rate of LIGO-Virgo sources from the stochastic gravitational wave background, *Mon. Not. Roy. Astron. Soc.* **501**, 2451 (2021), [arXiv:2006.03064 \[astro-ph.CO\]](#).
- [76] L. Lindblom, B. J. Owen, and D. A. Brown, Model Waveform Accuracy Standards for Gravitational Wave Data Analysis, *Phys. Rev. D* **78**, 124020 (2008), [arXiv:0809.3844 \[gr-qc\]](#).
- [77] M. Dominik, E. Berti, R. O’Shaughnessy, I. Mandel, K. Belczynski, C. Fryer, D. E. Holz, T. Bulik, and

- F. Pannarale, Double Compact Objects III: Gravitational Wave Detection Rates, *Astrophys. J.* **806**, 263 (2015), [arXiv:1405.7016 \[astro-ph.HE\]](#).
- [78] H.-Y. Chen, D. E. Holz, J. Miller, M. Evans, S. Vitale, and J. Creighton, Distance measures in gravitational-wave astrophysics and cosmology, *Class. Quant. Grav.* **38**, 055010 (2021), [arXiv:1709.08079 \[astro-ph.CO\]](#).
- [79] M. Maggiore *et al.*, Science Case for the Einstein Telescope, *JCAP* **03**, 050, [arXiv:1912.02622 \[astro-ph.CO\]](#).
- [80] M. Evans *et al.*, A Horizon Study for Cosmic Explorer: Science, Observatories, and Community, (2021), [arXiv:2109.09882 \[astro-ph.IM\]](#).
- [81] C. Talbot and E. Thrane, Measuring the binary black hole mass spectrum with an astrophysically motivated parameterization, *Astrophys. J.* **856**, 173 (2018), [arXiv:1801.02699 \[astro-ph.HE\]](#).
- [82] P. Madau and M. Dickinson, Cosmic Star Formation History, *Ann. Rev. Astron. Astrophys.* **52**, 415 (2014), [arXiv:1403.0007 \[astro-ph.CO\]](#).
- [83] R. Abbott *et al.* (KAGRA, VIRGO, LIGO Scientific), Population of Merging Compact Binaries Inferred Using Gravitational Waves through GWTC-3, *Phys. Rev. X* **13**, 011048 (2023), [arXiv:2111.03634 \[astro-ph.HE\]](#).
- [84] F. Iacovelli, M. Mancarella, S. Foffa, and M. Maggiore, Forecasting the Detection Capabilities of Third-generation Gravitational-wave Detectors Using GWFAST, *Astrophys. J.* **941**, 208 (2022), [arXiv:2207.02771 \[gr-qc\]](#).
- [85] F. Iacovelli, M. Mancarella, S. Foffa, and M. Maggiore, GWFAST: A Fisher Information Matrix Python Code for Third-generation Gravitational-wave Detectors, *Astrophys. J. Supp.* **263**, 2 (2022), [arXiv:2207.06910 \[astro-ph.IM\]](#).
- [86] A. Esteban-Gutiérrez, E. Mediavilla, J. Jiménez-Vicente, and J. A. Muñoz, Constraints on the Abundance of Primordial Black Holes from X-Ray Quasar Microlensing Observations: Substellar to Planetary Mass Range, *Astrophys. J.* **954**, 172 (2023), [arXiv:2307.07473 \[astro-ph.CO\]](#).
- [87] P. Mroz *et al.*, No massive black holes in the Milky Way halo, (2024), [arXiv:2403.02386 \[astro-ph.GA\]](#).
- [88] T. Blaineau *et al.*, New limits from microlensing on Galactic black holes in the mass range $10 M_{\odot} < M < 1000 M_{\odot}$, *Astron. Astrophys.* **664**, A106 (2022), [arXiv:2202.13819 \[astro-ph.GA\]](#).
- [89] M. Oguri, J. M. Diego, N. Kaiser, P. L. Kelly, and T. Broadhurst, Understanding caustic crossings in giant arcs: characteristic scales, event rates, and constraints on compact dark matter, *Phys. Rev. D* **97**, 023518 (2018), [arXiv:1710.00148 \[astro-ph.CO\]](#).
- [90] M. Zumalacarregui and U. Seljak, Limits on stellar-mass compact objects as dark matter from gravitational lensing of type Ia supernovae, *Phys. Rev. Lett.* **121**, 141101 (2018), [arXiv:1712.02240 \[astro-ph.CO\]](#).
- [91] J. B. Muñoz, E. D. Kovetz, L. Dai, and M. Kamionkowski, Lensing of Fast Radio Bursts as a Probe of Compact Dark Matter, *Phys. Rev. Lett.* **117**, 091301 (2016), [arXiv:1605.00008 \[astro-ph.CO\]](#).
- [92] P. D. Serpico, V. Poulin, D. Inman, and K. Kohri, Cosmic microwave background bounds on primordial black holes including dark matter halo accretion, *Phys. Rev. Res.* **2**, 023204 (2020), [arXiv:2002.10771 \[astro-ph.CO\]](#).
- [93] V. Kalogera *et al.*, The Next Generation Global Gravitational Wave Observatory: The Science Book, (2021), [arXiv:2111.06990 \[gr-qc\]](#).
- [94] D. Croon and S. Seviliano Muñoz, Cosmic microwave background constraints on extended dark matter objects, (2024), [arXiv:2403.13072 \[astro-ph.CO\]](#).
- [95] P. F. Hopkins, G. T. Richards, and L. Hernquist, An Observational Determination of the Bolometric Quasar Luminosity Function, *Astrophys. J.* **654**, 731 (2007), [arXiv:astro-ph/0605678](#).
- [96] A. Soltan, Masses of quasars, *Mon. Not. Roy. Astron. Soc.* **200**, 115 (1982).
- [97] J. Paynter, R. Webster, and E. Thrane, Evidence for an intermediate-mass black hole from a gravitationally lensed gamma-ray burst, *Nature Astron.* **5**, 560 (2021), [arXiv:2103.15414 \[astro-ph.HE\]](#).
- [98] X. Yang, H.-J. Lü, H.-Y. Yuan, J. Rice, Z. Zhang, B.-B. Zhang, and E.-W. Liang, Evidence for Gravitational Lensing of GRB 200716C, *Astrophys. J. Lett.* **921**, L29 (2021), [arXiv:2107.11050 \[astro-ph.HE\]](#).
- [99] Z. Kalantari, A. Ibrahim, M. R. R. Tabar, and S. Rahvar, Imprints of Gravitational Millilensing on the Light Curve of Gamma-Ray Bursts, *Astrophys. J.* **922**, 77 (2021), [arXiv:2105.00585 \[astro-ph.CO\]](#).
- [100] D. Croon, D. McKeen, and N. Raj, Gravitational microlensing by dark matter in extended structures, *Phys. Rev. D* **101**, 083013 (2020), [arXiv:2002.08962 \[astro-ph.CO\]](#).
- [101] P. W. Graham and H. Ramani, Constraints on Dark Matter from Dynamical Heating of Stars in Ultrafaint Dwarfs. Part 2: Substructure and the Primordial Power Spectrum, (2024), [arXiv:2404.01378 \[hep-ph\]](#).
- [102] A. Arvanitaki, S. Dimopoulos, M. Galanis, L. Lehner, J. O. Thompson, and K. Van Tilburg, Large-misalignment mechanism for the formation of compact axion structures: Signatures from the QCD axion to fuzzy dark matter, *Phys. Rev. D* **101**, 083014 (2020), [arXiv:1909.11665 \[astro-ph.CO\]](#).
- [103] P. Amaro-Seoane *et al.* (LISA), Laser Interferometer Space Antenna, (2017), [arXiv:1702.00786 \[astro-ph.IM\]](#).
- [104] P. Auclair *et al.* (LISA Cosmology Working Group), Cosmology with the Laser Interferometer Space Antenna, (2022), [arXiv:2204.05434 \[astro-ph.CO\]](#).
- [105] M. Çalıřkan, J. M. Ezquiaga, O. A. Hannuksela, and D. E. Holz, Lensing or luck? False alarm probabilities for gravitational lensing of gravitational waves, (2022), [arXiv:2201.04619 \[astro-ph.CO\]](#).
- [106] B. Zhou, L. Reali, E. Berti, M. Çalıřkan, C. Creque-Sarbinowski, M. Kamionkowski, and B. S. Sathyaprakash, Subtracting compact binary foregrounds to search for subdominant gravitational-wave backgrounds in next-generation ground-based observatories, *Phys. Rev. D* **108**, 064040 (2023), [arXiv:2209.01310 \[gr-qc\]](#).
- [107] B. Zhou, L. Reali, E. Berti, M. Çalıřkan, C. Creque-Sarbinowski, M. Kamionkowski, and B. S. Sathyaprakash, Compact Binary Foreground Subtraction in Next-Generation Ground-Based Observatories, (2022), [arXiv:2209.01221 \[gr-qc\]](#).
- [108] H. Zhong, R. Ormiston, and V. Mandic, Detecting cosmological gravitational wave background after removal of compact binary coalescences in future gravitational wave detectors, *Phys. Rev. D* **107**, 064048 (2023), [Erratum: *Phys.Rev.D* 108, 089902 (2023)], [arXiv:2209.11877 \[gr-qc\]](#).

- [109] R. Dey, L. F. Longo Micchi, S. Mukherjee, and N. Afshordi, Spectrogram correlated stacking: A novel time-frequency domain analysis of the stochastic gravitational wave background, *Phys. Rev. D* **109**, 023029 (2024), [arXiv:2305.03090 \[gr-qc\]](#).
- [110] G. F. Lewis, Gravitational Microlensing Time Delays at High Optical Depth: Image Parities and the Temporal Properties of Fast Radio Bursts, *Mon. Not. Roy. Astron. Soc.* **497**, 1583 (2020), [arXiv:2007.03919 \[astro-ph.CO\]](#).
- [111] L. L. R. Williams and R. A. M. J. Wijers, Distortion of gamma-ray burst light curves by gravitational microlensing, *Mon. Not. Roy. Astron. Soc.* **286**, L11 (1997), [arXiv:astro-ph/9701246 \[astro-ph\]](#).
- [112] J. M. Diego, O. A. Hannuksela, P. L. Kelly, T. Broadhurst, K. Kim, T. G. F. Li, G. F. Smoot, and G. Pagano, Observational signatures of microlensing in gravitational waves at LIGO/Virgo frequencies, *Astron. Astrophys.* **627**, A130 (2019), [arXiv:1903.04513 \[astro-ph.CO\]](#).
- [113] A. Mishra, A. K. Meena, A. More, S. Bose, and J. S. Bagla, Gravitational lensing of gravitational waves: effect of microlens population in lensing galaxies, *Mon. Not. Roy. Astron. Soc.* **508**, 4869 (2021), [arXiv:2102.03946 \[astro-ph.CO\]](#).
- [114] A. K. Meena, A. Mishra, A. More, S. Bose, and J. S. Bagla, Gravitational lensing of gravitational waves: Probability of microlensing in galaxy-scale lens population, *Mon. Not. Roy. Astron. Soc.* **517**, 872 (2022), [arXiv:2205.05409 \[astro-ph.GA\]](#).
- [115] M. H. Y. Cheung, J. Gais, O. A. Hannuksela, and T. G. F. Li, Stellar-mass microlensing of gravitational waves, *Mon. Not. Roy. Astron. Soc.* **503**, 3326 (2021), [arXiv:2012.07800 \[astro-ph.HE\]](#).
- [116] S. M. C. Yeung, M. H. Y. Cheung, J. A. J. Gais, O. A. Hannuksela, and T. G. F. Li, Microlensing of type II gravitational-wave macroimages, (2021), [arXiv:2112.07635 \[gr-qc\]](#).
- [117] X. Shan, G. Li, X. Chen, W. Zheng, and W. Zhao, Wave effect of gravitational waves intersected with a microlens field: A new algorithm and supplementary study, *Sci. China Phys. Mech. Astron.* **66**, 239511 (2023), [arXiv:2208.13566 \[astro-ph.CO\]](#).
- [118] X. Shan, X. Chen, B. Hu, and R.-G. Cai, Microlensing sheds light on the detection of strong lensing gravitational waves, (2023), [arXiv:2301.06117 \[astro-ph.IM\]](#).
- [119] X. Shan, X. Chen, B. Hu, and G. Li, Microlensing bias on the detection of strong lensing gravitational wave, (2023), [arXiv:2306.14796 \[astro-ph.CO\]](#).
- [120] A. K. Meena, Gravitational Lensing of Gravitational Waves: Probing Intermediate Mass Black Holes in Galaxy Lenses with Global Minima, (2023), [arXiv:2305.02880 \[astro-ph.CO\]](#).
- [121] B. J. Kavanagh, [bradkav/PBHbounds: Release version](#), Zenodo (2019).
- [122] T. P. Robitaille *et al.* (Astropy), Astropy: A Community Python Package for Astronomy, *Astron. Astrophys.* **558**, A33 (2013), [arXiv:1307.6212 \[astro-ph.IM\]](#).
- [123] A. M. Price-Whelan *et al.* (Astropy), The Astropy Project: Building an Open-science Project and Status of the v2.0 Core Package, *Astron. J.* **156**, 123 (2018), [arXiv:1801.02634](#).
- [124] A. M. Price-Whelan *et al.* (Astropy), The Astropy Project: Sustaining and Growing a Community-oriented Open-source Project and the Latest Major Release (v5.0) of the Core Package*, *Astrophys. J.* **935**, 167 (2022), [arXiv:2206.14220 \[astro-ph.IM\]](#).
- [125] C. R. Harris and *et al.*, Array programming with NumPy, *Nature* **585**, 357 (2020).
- [126] P. Virtanen and *et al.*, SciPy 1.0: Fundamental Algorithms for Scientific Computing in Python, *Nature Methods* **17**, 261 (2020).